THE JOURNAL OF PHYSICAL CHEMISTRY A

Article

pubs.acs.org/JPCA

A Quantum Mechanical Study of the $k-j$ and $k'-j'$ Vector Correlations for the H + LiH → Li + H_2 Reaction

Ahmad W. Huran,[†,‡] L. González-Sánchez,[†] S. Gomez-Carrasco,[†] and J. Aldegunde*[,†]

[†]Departamento de Química Física, Facultad de Ciencias Químicas, University of Salamanca, 37008 Salamanca, Spain

[‡]Instituto de Ciencia Molecular, Universidad de Valencia, 46890 Paterna, Spain

Supporting Information

ABSTRACT: We have characterized the stereodynamics of the H + LiH (v = 0, j = 0−1) reactive collisions leading to H_2 formation through the quantum mechanical analysis of the $k-j$ and $k'-j'$ vector correlations that describe the polarization of the reactants and products, respectively. Our results, which cover the collision energy interval between 10^{-4} and 1 eV, are unexpectedly complex given the apparent simplicity and featureless nature of the potential energy surface for the LiH_2 system and point toward the existence of a dynamical barrier connected to the centrifugal barrier. Both reactants and products, in particular the second ones, display strong directional preferences in the cold region that indicate a bias for collinear approaching and departing geometries and are independent of the final state of the products. As more energy is available for the reaction, the polarization of reactants and products becomes weaker and strongly dependent on the final state. While stereodynamical control is feasible and significant in the cold region, its extent becomes negligible for other energetic regimes.

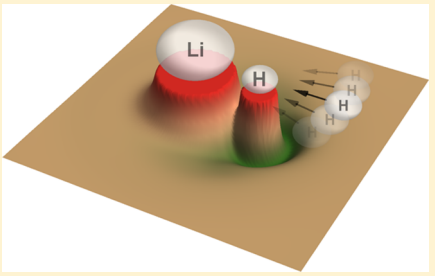

1. INTRODUCTION

The last decades have witnessed an increase in interest for the electronic and dynamical properties of the LiH_2 system.[1−10] The small number of electrons forming this system makes possible to perform highly accurate electronic-structure and dynamical calculations. The relevance of these calculations is not only limited to the exploration and understanding of the mechanism and dynamics of elementary reactions, but it also has its roots in the important role played by the LiH molecule in studies about the early universe,[1−3,6,7] where the

$$H + LiH \rightarrow Li + H_2 \quad (1)$$

reaction is thought to have contributed significantly to its depletion. Besides, alkali-dyhidrogen systems are known to possess densely packed electronic states,[11] which makes them the ideal testing ground for theoretical and experimental studies on nonadiabatic effects.[12]

The development of increasingly better potential energy surfaces (PESs) for the LiH_2 system was central to all studies concerning the properties of reaction 1 or its reverse. Clarke et al.[4] employed reduced dimensionality to build the surface corresponding to the ground electronic state and depicted the H + LiH reactive collisions as highly exothermic and influenced by the presence of a barrier in the reactant valley. The first three-dimensional surface for the LiH_2 system was generated by Dunne et al.[5] and, while exothermic, it did not display any barrier in the reactant valley. Further improvements in the fully dimensional surface for the ground electronic state of the LiH_2 system agreed in the exothermic nature of reaction 1 but led to contradictory results regarding the existence of the early staged barrier; it was absent in the surfaces due to Wernli et al.[8] and Yuan et al.[10] and present in the one of Prudente et al.[9] The analysis of Gómez-Carrasco et al.[13] settled the question by proving this last surface to have spurious structures due to the fitting procedure that caused the barrier to appear and lead to a significantly different dynamical behavior.

Accordingly, we will restrict our analysis to those dynamical studies[14−18] based on the barrierless PESs by Wernli et al.[8] and Yuan et al.,[10] as they produce consistent pictures[10] of the dynamics of reaction 1 except at low collision energies, when the process becomes more sensitive to the surface nuances. Such dynamical studies[14−18] were mainly devoted to the calculation of scalar properties,[19] that is, reaction probabilities and integral cross sections (ICSs), for H + LiH reactive collisions on the ground electronic state, as they make possible to evaluate the rate coefficients required by early universe molecular models.[1−3,6,7]

Compared to scalar observables, and exceptions notwithstanding,[10,13,14,18] the mechanism of reaction 1 and the vectorial observables[19] more directly connected to it have received little attention. However, it is possible to extract an overall picture of the mechanism behind the H + LiH reactive collisions from the studies already available in the literature. According to these studies, such collisions are direct[14] and not mediated by any kind of complex, occur preferably when the incoming atom approaches the target molecule[8] from the hydrogen side, and give rise to differential cross sections (DCSs) which are predominantly sideways and forward.[10,14,18]

Received: October 5, 2016
Revised: February 2, 2017
Published: February 3, 2017

DOI: 10.1021/acs.jpca.6b10094
J. Phys. Chem. A 2017, 121, 1535−1543

In the most thorough analysis of the mechanism yet performed, He et al.[18] identified two mechanisms: a direct rebound one correlating with small values of the total angular momentum (J) and backward scattering and a stripping mechanism that is responsible for most of the reactivity, dominates the overall process, correlates with medium and large values of J, and accounts for the sideways and forward scattering.

The differential cross section is the simplest example of vector correlation as it informs about the relative arrangement adopted by the approach direction ($\boldsymbol{k}$) of the reactants and the recoil direction ($\boldsymbol{k}'$) of the products when the reaction takes place. Even for reactions for which all species are considered as closed shell there exist other vectorial properties which participate in the process: the rotational angular momenta of the reactants ($\boldsymbol{j}$) and products ($\boldsymbol{j}'$). The explicit consideration of these four vectors and the study of the correlations among them reveals aspects of the reaction mechanism that cannot be grasped only through the analysis of the differential cross section which, although extremely interesting, does not contain any information about the preferred arrangements adopted by reactants or products. Although different studies[20−25] have focused on the analysis of such correlations for the two reactive channels of the H + LiH collisions, with special emphasis on the $\boldsymbol{k}-\boldsymbol{k}'-\boldsymbol{j}'$ combination, all of them were based on quasiclassical trajectories calculations[19] performed on the surface by Prudente et al.[9] The goal of this work is to complement previous studies by presenting a quantum mechanical description of the stereodynamics of reaction 1 on a different potential energy surface. In particular, we will concentrate on the $\boldsymbol{k}-\boldsymbol{j}$ and $\boldsymbol{k}'-\boldsymbol{j}'$ correlations and will use the surface of Wernli et al.[8] for the scattering calculations. The consideration of the polarization of the reactants through the $\boldsymbol{k}-\boldsymbol{j}$ correlation is particularly convenient as, besides providing information about the mechanism, it makes possible an assessment of the sensibility of the reaction to different experimental preparations of the reactants.[26]

The substantial differences between the reaction probabilities[13] and the quasiclassical polarizations[27] calculated on the two surfaces mentioned in the former paragraph justify the necessity of performing an analysis of the mechanism on the potential by Wernli et al.[8] Besides, the results we present for reaction 1 are novel from different points of view. First, they represent the first quantum mechanical description of vector correlations other than the DCS. Second, and to the best of our knowledge, the polarization ($\boldsymbol{k}-\boldsymbol{j}$ correlation) of the reactants had never been studied before. Lastly, we present the first systematic description of the stereodynamics dependence with the final state of the products for the title reaction.

The paper is organized as follows. In section 2 we will use the H + LiH(v = 0, j = 1) reactive collisions leading to H_2 formation to illustrate the general dynamical features of reaction 1. The j = 1 state has been selected because former studies on the LiH_2 system mainly focus on rotationless reactants. The mathematical formalism necessary to quantify the $\boldsymbol{k}-\boldsymbol{j}$ and $\boldsymbol{k}'-\boldsymbol{j}'$ correlations as well as the analysis of the directional information they contain is presented in sections 3 and 4, respectively. While in section 3 we will consider the H + LiH(v = 0, j = 1) collisions in order to illustrate the features of the polarization of the reactants, section 4 will use the H + LiH(v = 0, j = 0) reaction to characterize the polarization of the products. Finally, the main results of the work are summarized in section 5.

2. GENERAL FEATURES OF THE H + LIH → LI + H_2 COLLISIONS

We first present a general overview of the dynamics of the H + LiH → Li + H_2 collisions which will serve the double purpose of complementing other studies[13,18] that focus on rotationless reactants and laying down the background for the analysis of the reaction stereodynamics unfolded in sections 3 and 4. All the results discussed in this and the following sections are based on quantum mechanical scattering calculations performed on the PES developed by Wernli et al.[8] The correct long-range description of the interactions was included in the PES, ensuring the good behavior of the potential even in the limit of low collision energies. The wavepacket methodology used in the scattering calculations and the values of the parameters necessary to attain convergence were the same presented in refs 13 and 28 and will not be described here for the sake of brevity.

The state-to-state integral cross section for the H + LiH (v, j) → Li + H_2 (v', j') collisions is given by

$$\sigma = \frac{\pi}{k_{vj}^{\,2}(2j+1)} \sum_{J} (2J+1) \sum_{\Omega=-\min(J,j)}^{\min(J,j)} \sum_{\Omega'=-\min(J,j')}^{\min(J,j')} |S^{EJ}_{v'j'\Omega',vj\Omega}|^2 \tag{2}$$

where $S^{EJ}_{v'j'\,\Omega',v\,j\,\Omega}$ represents the scattering matrix elements that form the outcome of the scattering calculations and where E indicates the total energy, J holds for the total angular momentum quantum number and Ω (Ω') are the helicity of the reactants (products), that is, the projection of the rotational angular momentum $\boldsymbol{j}$ ($\boldsymbol{j}'$) of the reactants (products) on the H−LiH approach (Li−H_2 recoil) direction. The constant $k_{v\,j}$ is given by

$$k_{vj}^{\,2} = \frac{2\mu}{\hbar^2} E_{\mathrm{coll}} \tag{3}$$

where μ represents the reduced mass of the H−LiH system and E_{coll} is the collision energy.

As a first illustration of the dynamical properties of the title reaction, Figure 1 shows the integral cross section summed over final rotational states (vibrationally resolved excitation functions) for the H + LiH (v = 0, j = 1) encounters leading to H_2 (v' = 0−5) formation and collision energies compressed in the 10^{-4} to 1 eV interval. The excitation functions display

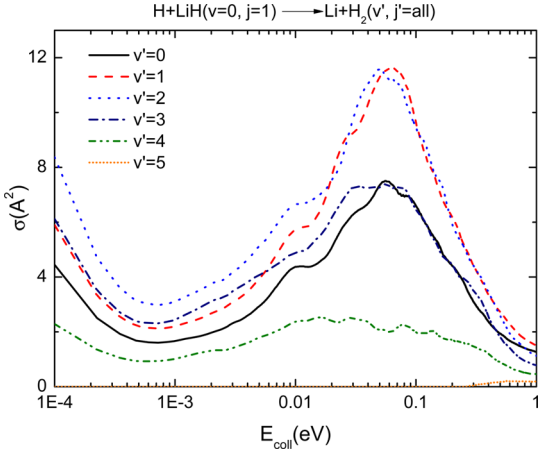

Figure 1. Vibrationally resolved excitation functions for the H + LiH (v = 0, j = 1) → Li + H_2 (v' = 0−5, j' = all) reactions. The results are similar to those published in ref 13 for rotationless reactants.

DOI: 10.1021/acs.jpca.6b10094
J. Phys. Chem. A 2017, 121, 1535−1543

similar profiles regardless of v', their values indicate the existence of population inversion and no threshold energy exists except for $v' = 5$. The highest reactivity corresponds to the $v' = 1$ and 2 states as well as to $v' = 3$ at the lowest energies considered. The results are similar to those obtained for rotationless reactants[13] and, as in that case, suggest a complex reaction mechanism regarding vibrational excitation. As the collision energy diminishes and the ultracold limit is approached, the shape of the excitation functions comes to be determined by the Wigner laws[29] and they approach parallel lines with slope proportional to $E_{coll}^{-1/2}$.

The state-to-state reaction probabilities as a function of the total angular momentum quantum number J are given by

$$P(J) = \frac{1}{2\min(J, j) + 1} \sum_{\Omega\Omega'} |S^{EJ}_{v'j'\Omega',vj\Omega}|^2 \quad (4)$$

Figure 2 shows the total (summed over all final states) reaction probabilities for the H + LiH ($v = 0$, $j = 1$) reaction as a

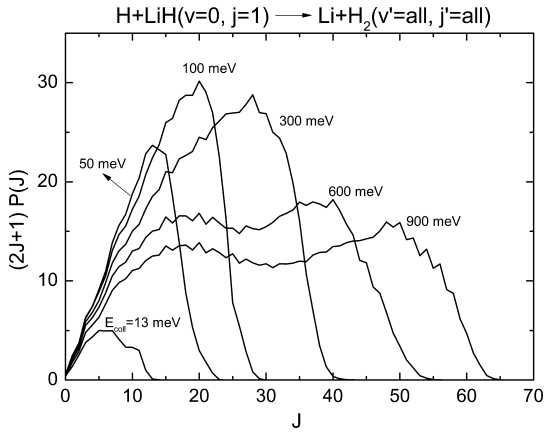

Figure 2. Total, summed over final states, reaction probability as a function of the total angular momentum quantum number (J) and multiplied by ($2J + 1$) for the H + LiH ($v = 0$, $j = 1$) → Li + H_2 (v' = all, j' = all) reaction at different values of the collision energy.

function of the collision energy. The probabilities have been multiplied by ($2J + 1$) in order to reflect the contribution of each value of J to the integral cross section (see eq 2). When $j = 1$, the total angular momentum $\boldsymbol{J}$ can be considered almost identical to the orbital angular momentum $\boldsymbol{L}$ of the reactants and, therefore, proportional to the classical impact parameter. Collision energies up to 300 meV correlate with $(2J + 1)\cdot P(J)$ curves that are slightly asymmetric and dominated by the largest values of J accessible at each energy; they display a linear increase with J up to a maximum followed by an abrupt fall to zero. For larger collision energies, the curves become progressively wider and flatter while developing a plateau that stretches over most of the J range. Under these circumstances, the relative importance of the largest values of J gets smaller. Results presented in Figure 2 are in good accordance with the mechanistic analysis of the H + LiH reaction performed by He et al.[18] for rotationless reactants; in the range of collision energies studied, up to 0.6 eV, the authors found the collisions to be dominated by a stripping mechanism giving rise to forward scattering and corresponding to medium and large values of J.

Figure 3 shows the breakdown of the reaction probability into v' contributions. Except at the lowest collision energies (top panel in Figure 3), where the maximum number of partial

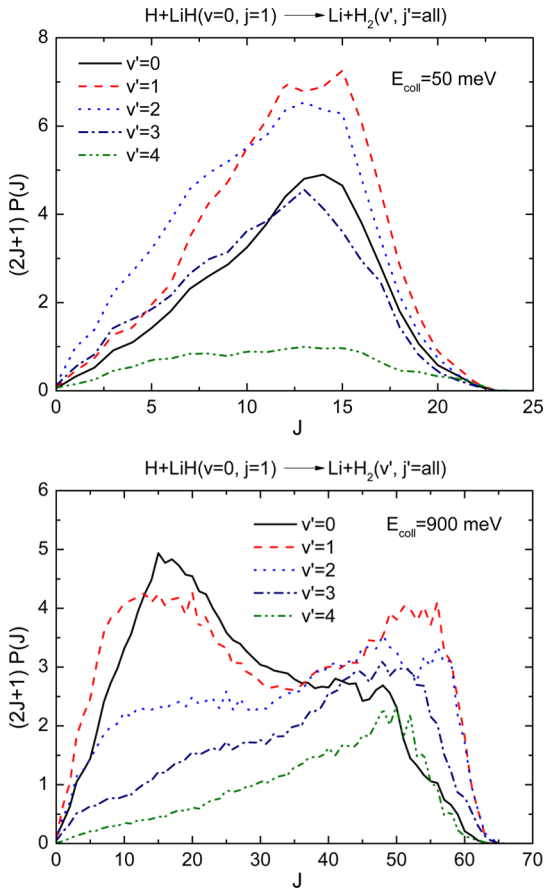

Figure 3. Vibrationally resolved reaction probability as a function of the total angular momentum quantum number (J) and multiplied by ($2J + 1$) for the H + LiH ($v = 0$, $j = 1$) → Li + H_2 ($v' = 0$–4, j' = all) reactions at E_{coll} = 50 and 900 meV.

waves is severely limited by the centrifugal barrier and the shape of the curves is independent of the vibrational excitation of the products, the probability functions changed significantly with v'. Such changes are exemplified by the E_{coll} = 900 meV case (bottom panel in Figure 3) and can be summarized by saying that, while $v' = 0$ collisions are dominated by small/medium J values, the vibrational excitation of the products correlates with an increase of the importance of the largest partial waves and with a shifting of the curves to the right. This trend also agrees with the analysis performed by He et al.,[18] whose results suggest that the preeminent role of the stripping mechanism, the one connected to the largest values of J, was more evident for vibrationally excited products.

The rotational distributions, state-to-state integral cross sections as a function of the products' rotational quantum number j', for the H + LiH($v = 0$, $j = 1$) collisions leading to H_2 formation are presented in the Supporting Information file. Their features are qualitatively identical to their counterparts for rotationless reactants obtained by Gómez-Carrasco et al.[13]

3. REACTANTS ALIGNMENT AND STEREODYNAMICAL CONTROL: THE *k*–*j* CORRELATION

The analysis of the two-vectors correlations[30] represents the simplest approach to the study of a reaction stereodynamics. Among these, and leaving aside the differential cross section, the $\boldsymbol{k}$–$\boldsymbol{j}$ correlation[30] is the foremost one as the information it

DOI: 10.1021/acs.jpca.6b10094
J. Phys. Chem. A 2017, 121, 1535–1543

contains is easy to interpret and to express in quantitative terms and because it makes it possible to evaluate the extent to which the reaction is amenable to stereodynamical control. In particular, the $k-j$ correlation measures the relative arrangement between the approach direction (k) and the rotational angular momentum (j) of the reagents when the reaction takes place. In this section, we will describe its characteristics for the H + LiH ($v = 0$, $j = 1$) collisions leading to H_2 formation.

As for any other reaction property, the quantum mechanical features of the $k-j$ correlation can be extracted from the scattering matrix elements. Specifically, the quantitative details of this vector correlation are condensed into a set of polarization moments[31] called polarization parameters[32] such that, for the H + LiH ($v = 0$, $j = 1$) → Li + H_2 (v', j') state-to-state reaction, only the one indicated as PP_r (2, 0) is relevant for the analysis of the reaction mechanism averaged over the whole range of scattering angle values. This moment can be evaluated through

$$PP_r(2,0) = \frac{1}{N}\sum_J (2J+1)\sum_{\Omega}\sum_{\Omega'} |S^{EJ}_{v'j'\Omega',vj\Omega}|^2 \langle j\Omega 20|j\Omega\rangle \quad (5)$$

where the N factor is given by

$$N = \sum_J (2J+1)\sum_{\Omega}\sum_{\Omega'} |S^{EJ}_{v'j'\Omega',vj\Omega}|^2 \quad (6)$$

$\langle\cdots|\cdots\rangle$ represents a Clebsch−Gordan coefficient and the $PP_r(2,0)$ values so obtained possess the following directional interpretation:[32] positive figures indicate that j and k tend to be aligned parallel while negative figures correlate with collision geometries in which both vectors adopt a perpendicular configuration. The opposite applies if one considers the internuclear axis r; positive/negative values of $PP_r(2,0)$ point to a preference for collisions where r and k are perpendicular/parallel, that is, to side-on and head-on collisions, respectively. In a quantum mechanical context, the range of values that $PP_r(2,0)$ can take is determined[26] by the j quantum number that defines the rotational state of the reactant molecule, in such a way that the aforementioned directional preferences will be more accentuated as the value of the polarization moment gets closer to any of the interval limits. For the $j = 1$ case, this range is $[-0.632,0.316]$.

The state-to-state $PP_r(2,0)$ can be averaged[32] using the state-to-state integral cross sections as weights in order to obtain vibrationally resolved values of the moment that describe the $k-j$ correlation for the H + LiH ($v = 0$, $j = 1$) → Li + H_2 (v', j' = all) collisions. The values of $PP_r(2,0)$ so calculated for $v' = 0-4$ are presented in Figure 4 as a function of the collision energy. It is possible to differentiate several regions in this figure as the collision energy increases. At very low energies, near the ultracold limit, the values of the moment tend to zero irrespectively of the final state as the $l = 0$ partial wave remains the only one contributing to reactivity. This behavior is general[33,34] for all chemical reactions when $E_{coll} \to 0$. Getting further from the ultracold limit correlates with increasingly negative values of the moment until reaching a minimum around $E_{coll} = 2 \times 10^{-3}$ eV. This indicates a preference for head-on collisions that is independent of the v' state, as the different curves are almost coincident. From this minimum, the evolution of the vibrationally resolved $PP_r(2,0)$ becomes different; while for $v' = 0$ the moment increases until stabilizing slightly above zero, the rise is less pronounced as v' gets larger

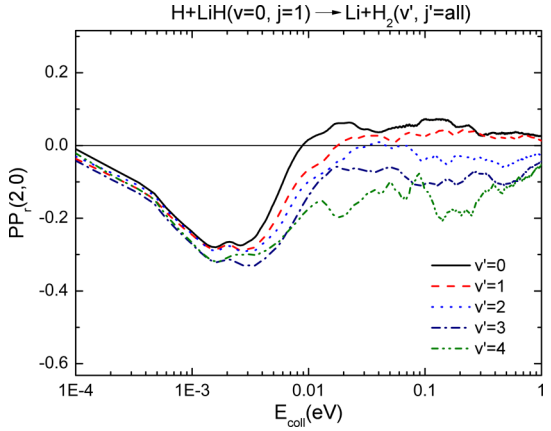

Figure 4. Vibrationally resolved $PP_r(2,0)$ moments for the H + LiH ($v = 0$, $j = 1$) → Li + H_2($v' = 0-4$, j' = all) reactions as a function of the collision energy. The y-axis scale corresponds to the quantum mechanical limits of the polarization parameter for $j = 1$, i.e., $[-0.632,0.316]$.

and the plateau is reached at increasingly more negative values. In other words, once the ultracold and cold regions are left behind $v' = 0$ products display a weak preference for side-on approaching geometries and highly excited products for head-on collisions. Although this seems to agree with the widespread picture that correlates vibrational excitation in direct reactions with head-on collisions that proceed through a compression of the reagents bond followed by a cleavage of the reaction intermediate, such a model[35] does not reflect the complexity of the mechanism behind the vibrational excitation for the target reaction. In the first place, the values of the $PP_r(2,0)$ moment above 10^{-2} eV are clustered relatively near to zero, indicating that the directional preferences are weak. Besides, Figure 3 shows how the highest v' states are populated through collisions characterized by the largest impact parameters, just the opposite to what one would expect if the aforementioned model were valid.

Deeper insight into the collisions mechanism can be attained through the state-to-state values of $PP_r(2,0)$, which are presented in Figure 5 for the H + LiH ($v = 0$, $j = 1$) → Li + H_2 ($v' = 1-2$, j') reactions at four collision energies (2, 50, 300, and 600 meV). Our discussion will only consider the $v' = 1$ and 2 states as they suffice to illustrate the evolution followed by the state-to-state $PP_r(2,0)$ as a function of v' while concentrating the major contribution to the reactivity (see Figure 1). Regardless of the v' state and collision energy considered, the $PP_r(2,0)$ moment always shifts from negative values to less negative or even positive values as j' increases, indicating a head-on character of the collisions that weakens or even turns slightly side-on as the products become rotationally excited. While for energies located in the cold region (E_{coll} = 2 meV in Figure 5) the values of $PP_r(2,0)$ are strongly negative irrespectively of j', above that region they become less negative, in particular for medium and large j' states, and the plots turn almost independent of the energy. Interestingly, if one considers the curves for a fixed value of the energy, it is found that they experience a displacement as a whole toward more negative values as v' increases. This result is behind the evolution of the vibrationally resolved moments presented in Figure 4 and shows how the shift they display toward negative values as v' increases can not be traced back to a group of rotational states but to the totality of them.

DOI: 10.1021/acs.jpca.6b10094
J. Phys. Chem. A 2017, 121, 1535−1543

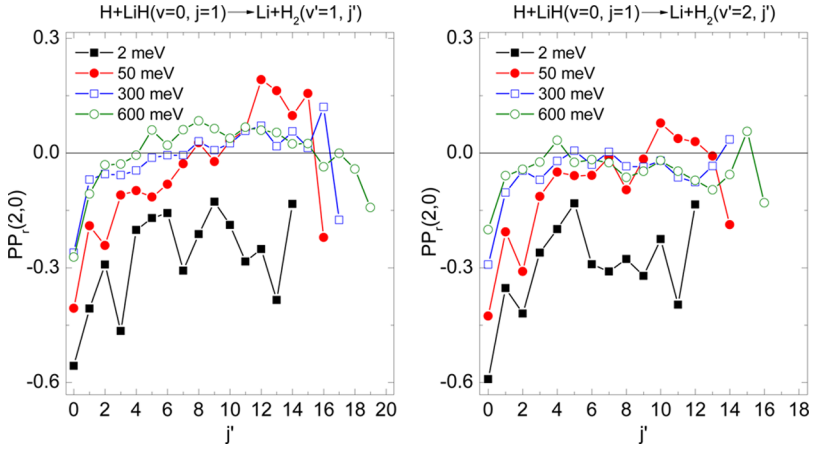

Figure 5. State-to-state $PP_r(2,0)$ moments for the H + LiH (v = 0, j = 1) → Li + H_2 (v'=1−2, j') reactions at E_{coll} = 2, 50, 300, and 600 meV. The y-axis scale corresponds to the quantum mechanical limits of the polarization parameter for j = 1, i.e., [−0.632,0.316].

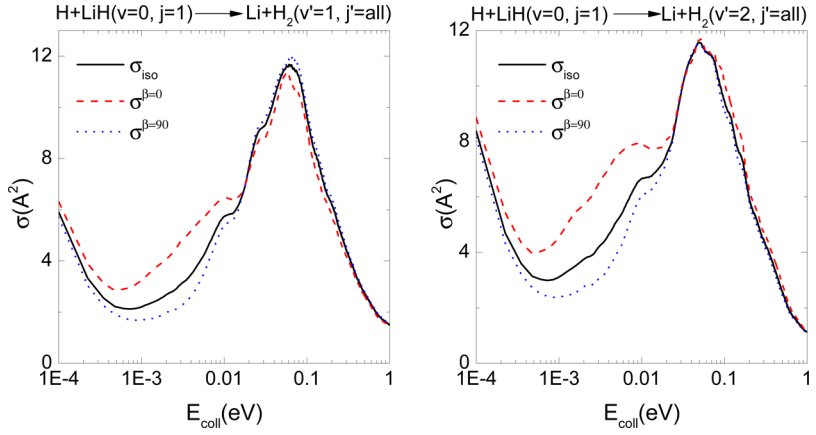

Figure 6. Excitation function for the H + LiH (v = 0, j = 1) → Li + H_2 (v' = 1−2, j' = all) reactions for unpolarized (σ_{iso}) and polarized ($\sigma^{\beta=0^\circ}$ and $\sigma^{\beta=90^\circ}$) reactants.

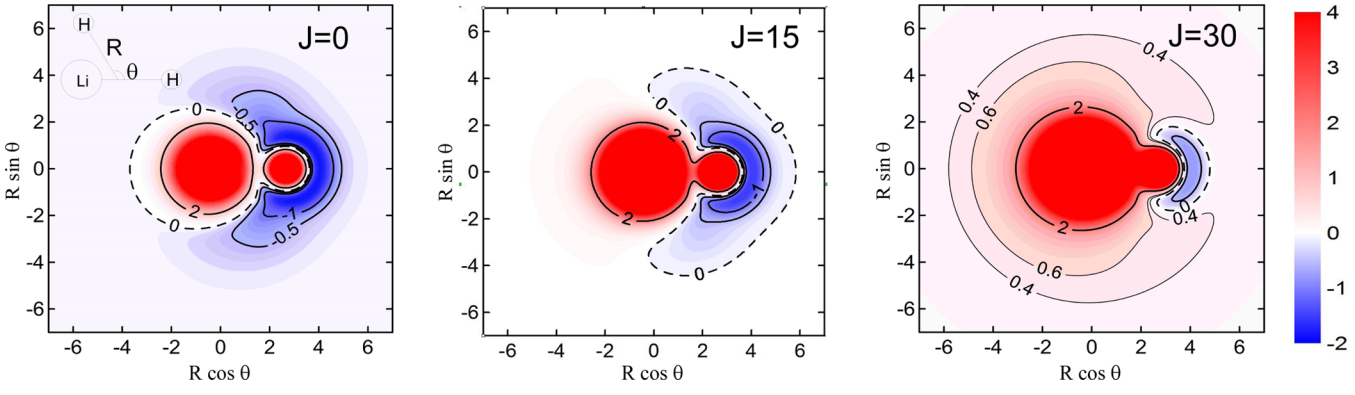

Figure 7. Plot of the potential obtained by summing the energy surface by Wernli et al.[8] to the centrifugal barrier for three different values of the total angular momentum quantum number J (J = 0 (left), 15 (center), and 30 (right)). In all cases, the potentials correspond to the entrance valley of the H + LiH collisions because the internuclear distance of the reactant LiH molecule is kept constant at its equilibrium value (3.04 Bohr). The energy contours (in eV) are plotted as a function of R cos θ and R sin θ, the Cartesian components (in Bohr) of the atom−diatom (H−LiH) center of mass Jacobi vector. The reactant LiH molecule lies on the x axis with its center of mass at the origin. The zero of energy corresponds to the asymptote of the reactants and the isopotential curve for 0 eV is highlighted by means of a dashed line.

Besides containing stereodynamical information about the mechanism of a reaction, the polarization parameters measure the sensitivity of the integral cross section to the experimental preparation of the reactants;[32] the closer is the value of $PP_r(2,0)$ to its lower or upper limit the larger is the extent of the change in reaction probability caused by the polarization of the reactants prior to the collision. Those experimental arrangements that reflect the directional preferences of a reaction as expressed through the polarization parameters will increase the reactivity. On the contrary, a preparation that fails to mirror the reaction requirements will lead to a reactivity decrease. A brief description of the methodology necessary to quantify these

DOI: 10.1021/acs.jpca.6b10094
J. Phys. Chem. A 2017, 121, 1535−1543

directional effects is presented in the Supporting Information file.

The values of the $PP_r(2,0)$ presented in Figure 4 suggest that the dependence of the excitation functions on the experimental preparation of the reactants will be null in the ultracold limit, where the moment vanishes, significant in the cold region, where the moment is large and negative, and will decrease as the collision energy increases above 0.01 eV and the values of the moment become small. Figure 6 confirms this by displaying the cross sections for vibrationally resolved collisions leading to the formation of H_2 in the $v' = 1$ and 2 states when the reactants are unpolarized (σ_{iso}) and for two polarizations of the reactants that correspond to head-on ($\sigma^{\beta=0^\circ}$) and side-on ($\sigma^{\beta=90^\circ}$) collisions. The only appreciable changes in reactivity are found in the cold region, where the head-on preparation leads to noticeable increments in the reactivity and the side-on preparation hinders the process. The modifications experienced by the rotational distributions for the same preparations are similar to those displayed by the excitation functions (see the Supporting Information file).

Finding a strong dependence of the reactivity on the preparation of the reactants in the cold region is common for direct reactions with a barrier,[33] as the geometries accessible to the reactants are limited by the lack of energy available to surmount the electronic barrier. As the energy increases, the cone of acceptance gets wider and the sensitivity to the preparations of the reactants decreases significantly. However, for barrierless reactions one would not expect to find any significant stereodynamical control even at low collision energies, as all the approaching geometries could, at least in principle, reach the product valley. From this point of view, our results for the H + LiH collisions are surprising and suggest the presence of a dynamical barrier that impairs the reaction for noncollinear geometries in the cold region. As the energy increases its influence vanishes faster than for a reaction displaying an electronic barrier, leading to a very weak stereodynamical control. To clarify the origin of the strong directional effect for cold collisions, we present in the left panel of Figure 7 the plot of the potential[8] used in the calculations when the internuclear distance of the reactant LiH molecule is frozen at its equilibrium value. For all the directions around the LiH molecule the potential is negative and, as the zero energy in the plot corresponds to the reactant asymptote, this implies that the incoming H atom could approach the target molecule following any direction regardless of its energy and no preferred collision geometry would exist. However, this situation changes drastically as soon as the centrifugal barrier comes into play, as illustrated by the center and right panels in Figure 7, where we add the centrifugal barrier for $J = 15$ (center) and 30 (left) to the purely electronic potential (left panel). For cold collisions, when E_{coll} is small, the centrifugal barrier forces the incoming H atom to approach the H side of the target molecule collinearly. This orientation of the incoming atom by the surface, which is more intense the larger is the centrifugal barrier (larger J), leads to the strongly negative values of the $PP_r(2,0)$ moment and the preference for head-on approaches in the cold region.

4. PRODUCTS ALIGNMENT: THE $k'-j'$ CORRELATION

The information contained in the directional preferences of the reactants will be now complemented by the analysis of the alignment of the products. The most direct and intuitive description of this property is based on the $k'-j'$ correlation,[30] which measures the relative disposition adopted by the recoil direction (k') and the rotational angular momentum (j') of the products once the reaction has taken place. In this section we will analyze the directional information provided by this vector correlation for the H + LiH ($v = 0$, $j = 0$) collisions leading to H_2 formation. To this end, and following the procedure used in the $k-j$ case, we will concentrate on a single polarization parameter, $PP_p(2,0)$, whose state-to-state values are defined as follows

$$PP_p(2,0) = \frac{1}{N}\sum_J (2J+1)\sum_{\Omega'} |S^{EJ}_{v'j'\Omega',000}|^2 \langle j'\Omega'20|j'\Omega'\rangle$$
$$= \frac{1}{N}\left(C(0)\langle j'020|j'0\rangle + 2\sum_{\Omega'>0} C(\Omega')\langle j'\Omega'20|j'\Omega'\rangle\right) \quad (7)$$

where the N factor is given by eq 6 and the $C(\Omega')$ coefficients by

$$C(\Omega') = \sum_J (2J+1)|S^{EJ}_{v'j'\Omega',000}|^2 \quad (8)$$

This moment possesses properties which are analogue to those of $PP_r(2,0)$. First, positive (negative) values of $PP_p(2,0)$ correlate with geometries where j' and k' are parallel (perpendicular) and where the products' internuclear axes r' and k' are perpendicular (parallel). Besides, the quantum mechanical values of the moment are limited to well-defined intervals[26] the limits of which depend on j' and that, for medium and large values of this quantum number, tend to their classical counterparts ($[-0.5,1]$). To facilitate the interpretation of the results and to avoid the multiplicity of limits that stem from the consideration of the different rotational states of the products, all figures involving $PP_p(2,0)$ will use the classical limits to define the scale of the ordinate axis.

Figure 8 shows the vibrationally resolved values of $PP_p(2,0)$ for the H + LiH ($v = 0$, $j = 0$) → Li + H_2 ($v' = 0-4$, j' = all)

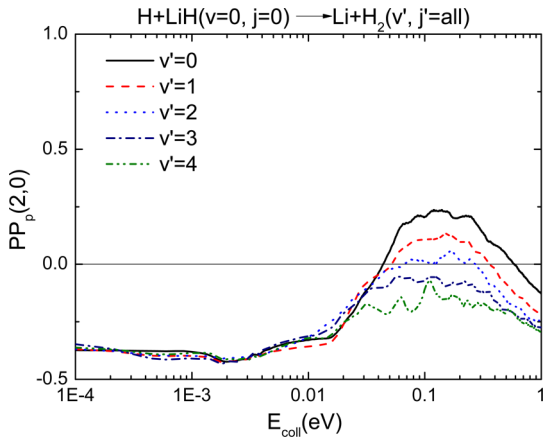

Figure 8. Vibrationally resolved $PP_p(2,0)$ moments for the H + LiH ($v = 0$, $j = 0$) → Li + H_2 ($v' = 0-4$, j' = all) reactions as a function of the collision energy. The y-axis scale corresponds to the classical limits of the polarization parameter, i.e., $[-0.5,1]$.

collisions obtained after averaging their state-to-state counterparts as in the $k-j$ case. For energies up to $\sim 2 \times 10^{-2}$ eV, $PP_p(2,0)$ is strongly negative, almost constant, and independent of v', indicating a very strong preference for collinear departing geometries where r' and k' are parallel. The proximity of the ultracold limit has no significant effect on the values of the

DOI: 10.1021/acs.jpca.6b10094
J. Phys. Chem. A 2017, 121, 1535−1543

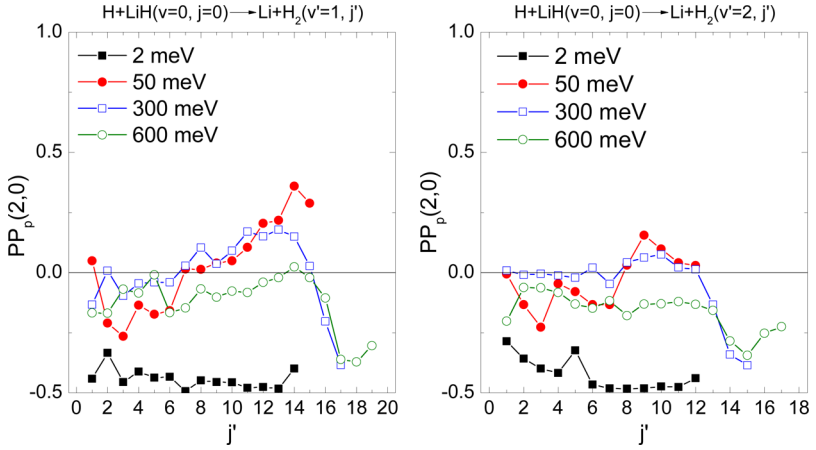

Figure 9. State-to-state $PP_p(2,0)$ moments for the H + LiH ($v = 0$, $j = 0$) → Li + H_2 ($v' = 1{-}2$, j') reactions at E_{coll} = 2, 50, 300, and 600 meV. The y-axis scale corresponds to the classical limits of the polarization parameter, i.e., [−0.5,1].

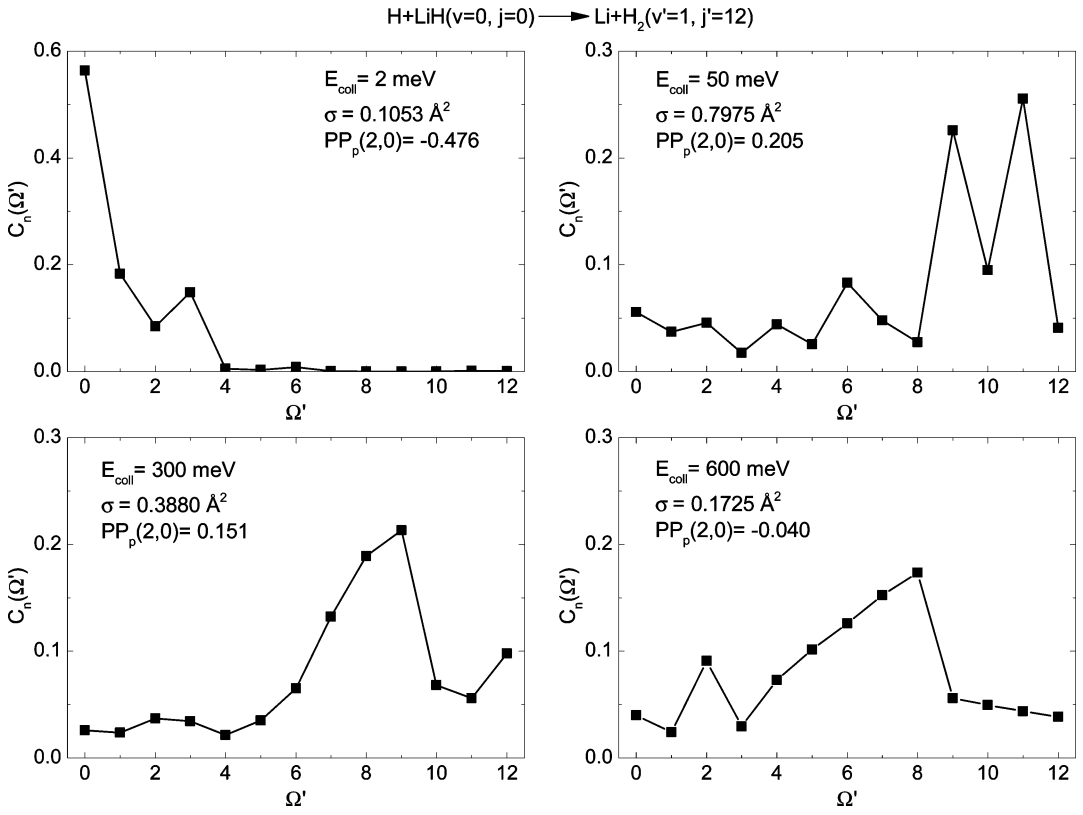

Figure 10. $C_n(|\Omega'|)$ coefficients for the H + LiH ($v = 0$, $j = 0$) → Li + H_2 ($v' = 1$, $j' = 12$) reaction at E_{coll} = 2, 50, 300, and 600 meV. The values of the state-to-state integral cross section (σ) and $PP_p(2,0)$ for each energy are included.

moment as, no matter how small E_{coll} is, the exothermicity of the reaction determines that the recoil energy of the products is always large and that many partial waves contribute to the asymptotic wave function of the products. For larger collision energies the different curves exhibit a bump, the height of which depends on v' and gets larger as this quantum number decreases. For $v' = 0$ products, and to a lower extent also for $v' = 1$, it causes the moment to become positive, indicating a slight preference for T-shaped recoil geometries. On the contrary, for $v' = 3$ and 4 the moment remains negative, although the preference for the collinear arrangement is weaker than at lower energies.

Following the same line of reasoning used in the analysis of the polarization of the reactants, Figure 9 shows the state-to-state $PP_p(2,0)$ for the H + LiH ($v = 0$, $j = 0$) → Li + H_2 ($v' = 1{-}2$, j') reactions as a function of j' and at the same four collision energies (2, 50, 300, and 600 meV) chosen for Figure 5. As in that case, the results for $v' = 1$ and 2 are representative of the behavior displayed by all the vibrational manifolds. The evolution of the state-to-state moment is strongly dependent on the energy. In the cold region (E_{coll} = 2 meV), the preference for collinear arrangements remains very strong regardless of j', although such a directional effect is slightly more intense for rotationally excited products, for which the values of the moment approach the lowest classical limit. For larger collision

DOI: 10.1021/acs.jpca.6b10094
J. Phys. Chem. A 2017, 121, 1535−1543

energies, the shapes of the curves change drastically. For small and medium j' states, the values of $PP_p(2,0)$ are clustered around zero, indicating that no significant alignment exists. Only when the collision energy gets high enough to make $j' > 12$ states energetically accessible does the alignment become intense, and again, collinear geometries are preferred for the departure of the products. Except in the cold region, where the vibrationally resolved moments were independent of v', the state-to-state plots corresponding to the same collision energy but increasingly larger v' states experience a shift toward negative values that mainly affects medium j' states and is behind the evolution discussed in connection to Figure 8. It is worth pointing out that, if the values of $PP_p(2,0)$ were normalized using their quantum mechanical limits, the profiles of the curves in Figure 9 would be qualitatively identical and the subsequent discussion about their meaning would be unchanged. The directional effects just described are therefore not affected by considering quantum mechanical or classical limits for the moments.

It is possible to shed additional light on the information contained in the polarization parameter $PP_p(2,0)$ by performing an analysis in terms of the values of the helicity Ω' of the products, the projection of the rotational angular momentum of the products ($\boldsymbol{j}'$) on their recoil direction $\boldsymbol{k}'$. The key to this analysis is eq 7 and, in particular, the coefficients $C(\Omega')$, which are always positive, possess the symmetry $C(\Omega') = C(-\Omega')$ and represent the contribution of a well-defined value of Ω' to the integral cross section (see eq 2). In particular, the value adopted by the moment $PP_p(2,0)$ corresponds to the sum of such coefficients weighted with the Clebsch-Gordan $\langle j'\Omega' 20| j'\Omega'\rangle$ which, in turn, is positive for absolute values of the helicity close to its limiting value j' and negative for helicities close to zero. In consequence, the sign and magnitude of $PP_p(2,0)$ reflects the predominance of large ($PP_p(2,0) > 0$) or small ($PP_p(2,0) < 0$) helicities which, in turn, correspond to side-on and head-on departing geometries.

As an example, Figure 10 presents values of the $C(\Omega')$ coefficients normalized according to

$$C_n(\Omega') = C(\Omega')/\sum_{\Omega'} C(\Omega') \tag{9}$$

for the H + LiH ($v = 0$, $j = 0$) → Li + H_2 ($v' = 1$, $j' = 12$) collisions at E_{coll} = 2, 50, 300, and 600 meV. Comparison with the values of the state-to-state $PP_p(2,0)$, also included in the figure, shows how significantly negative/positive moments correlate with small/large values of the helicity and, more importantly, how values of the moment close to zero originate from intermediate values of the helicity and not from a cancellation effect between large and small helicities. Although exemplified for a well-defined state-to-state reaction, these results are valid regardless of the final state and energy considered in this work.

5. CONCLUSION

Motivated by recent studies about the H + LiH → Li + H_2 reaction, we have analyzed the stereodynamics of these collisions using the $\boldsymbol{k}-\boldsymbol{j}$ and $\boldsymbol{k}'-\boldsymbol{j}'$ vector correlations. The polarization moments that characterize such correlations were calculated from the scattering matrices obtained from quantum mechanical scattering calculations performed on the most accurate potential energy surface nowadays available. To the best of our knowledge, the results presented constitute the first purely quantum mechanical analysis of the aforementioned vector correlations for the title reaction.

The rotational excitation of the reactants does not have a significant influence on the dynamics of the collisions. The products are preferably formed in high vibrational states and, unlike for most direct reactions, vibrational excitation correlates with larger values of the impact parameter, which hints toward a complicated mechanism for the population of these states.

The analysis of the vibrationally resolved results for the $\boldsymbol{k}-\boldsymbol{j}$ correlation shows that the alignment is particularly intense in the cold region, displaying a strong preference for head-on collisions. Given the absence of electronic barrier in the potential energy surface, this suggests the presence of a dynamical barrier that hinders the reaction for noncollinear geometries and whose origin can be traced back to the combined effect of a purely attractive but highly anisotropic potential energy surface and the centrifugal barrier. As more collision energy is available, the reaction becomes less sensitive to the approaching geometry and the mechanism becomes dependent on v'. State-to-state results show that, for all the vibrational manifolds, rotationless products strongly correlate with head-on collisions. As j' increases, such preference gets weaker and, except in the cold region, the values of the polarization moment get close to zero. The extent of the stereodynamical control achievable by controlling the preparation of the reactants reflects the values of the polarization moment and is only significant in the cold region.

The departing geometry of the products was analyzed both through the polarization moments that characterize the $\boldsymbol{k}'-\boldsymbol{j}'$ vector correlation and through the consideration of the contribution of each value of the product helicity to the reactivity. In general terms, the polarization is stronger for the products than for the reactants. Up to $E_{coll} = \sim 2 \times 10^{-2}$ eV, the products display a very strong preference for collinear geometries regardless of the value of v' and j'. For larger collision energies, the polarization of the products gets weaker and the preferred departing geometry becomes again dependent on the final state.

To sum up, our analysis shows that the mechanism of the H + LiH → Li + H_2 collisions is more complex than would be expected for a barrierless reaction. In spite of this fact, the anisotropic nature of the potential is enough to induce a rich dynamical behavior of a complexity similar to that observed for direct reactions possessing a barrier. We hope that this work will serve to encourage deeper dynamical and mechanistical studies of other barrierless reactions.

■ ASSOCIATED CONTENT

Supporting Information

The Supporting Information is available free of charge on the ACS Publications website at DOI: 10.1021/acs.jpca.6b10094.

A brief description of the methodology used to evaluate the stereodynamical control; the rotational distributions for the H + LiH($v = 0$, $j = 1$) → Li + H_2 collisions at several collision energies and for different preparations of the reactants (PDF)

■ AUTHOR INFORMATION

Corresponding Author

*E-mail: jalde@usal.es.

ORCID

J. Aldegunde: 0000-0003-4685-0126

DOI: 10.1021/acs.jpca.6b10094
J. Phys. Chem. A 2017, 121, 1535−1543

Notes

The authors declare no competing financial interest.

■ ACKNOWLEDGMENTS

We would like to thank the group of F. A. Gianturco for providing the PES. L.G-S. and J.A. acknowledge funding by the Spanish Ministry of Science and Innovation Grants No. CTQ2012-37404-C02, CTQ2015-65033-P, and Consolider Ingenio 2010 CSD2009-00038. A.W.H. acknowledges the support of the Erasmus Mundus programme of the European Union for his MC scholarship under the EPIC programme, and his MC TCCM scholarship regulated under the FPA 2010-0147. S.G-C. acknowledges funding by the Spanish Ministry of Economy and Competitiveness Grants No. FIS2014-52172-C2-2-P.

■ REFERENCES

(1) Lepp, S.; Shull, J. M. Molecules in the early Universe. *Astrophys. J.* **1984**, *280*, 465−469.
(2) Stancil, P.; Lepp, S.; Dalgarno, A. The lithium chemistry of the early universe. *Astrophys. J.* **1996**, *458*, 401−406.
(3) Bougleux, E.; Galli, D. Lithium hydride in the early universe and in protogalactic clouds. *Mon. Not. R. Astron. Soc.* **1997**, *288*, 638−648.
(4) Clarke, N.; Sironi, M.; Raimondi, M.; Kumar, S.; Gianturco, F.; Buonomo, E.; Cooper, D. Classical and quantum dynamics on the collinear potential energy surface for the reaction of Li with H_2. *Chem. Phys.* **1998**, *233*, 9−27.
(5) Dunne, L.; Murrell, J.; Jemmer, P. Analytical potential energy surface and quasi-classical dynamics for the reaction $LiH(X,^1\Sigma^+) + H(^2S) \rightarrow Li(^2S) + H_2(X,^1\Sigma^+)$. *Chem. Phys. Lett.* **2001**, *336*, 1−6.
(6) Lepp, S.; Stancil, P.; Dalgarno, A. Atomic and molecular processes in the early Universe. *J. Phys. B: At., Mol. Opt. Phys.* **2002**, *35*, R57−R80.
(7) Bodo, E.; Gianturco, F.; Martinazzo, R. The gas-phase lithium chemistry in the early universe: elementary processes, interaction forces and quantum dynamics. *Phys. Rep.* **2003**, *384*, 85−119.
(8) Wernli, M.; Caruso, D.; Bodo, E.; Gianturco, F. A. Computing a three-dimensional electronic energy manifold for the LiH + H→Li + H_2 chemical reaction. *J. Phys. Chem. A* **2009**, *113*, 1121−1128.
(9) Prudente, F. V.; Marques, J. M. C.; Maniero, A. M. Time-dependent wave packet calculation of the LiH plus H reactive scattering on a new potential energy surface. *Chem. Phys. Lett.* **2009**, *474*, 18−22.
(10) Yuan, J.; He, D.; Chen, M. A new potential energy surface for the ground electronic state of the LiH_2 system, and dynamics studies on the $H(^2S) + LiH(X^1\Sigma^+) \rightarrow Li(^2S) + H_2(X^1\Sigma^+)$ reaction. *Phys. Chem. Chem. Phys.* **2015**, *17*, 11732−11739.
(11) Lin, K.; Vetter, R. Alkali-hydrogen reactions. *Int. Rev. Phys. Chem.* **2002**, *21*, 357−383.
(12) Baer, M. *Beyond Born-Oppenheimer: electronic nonadiabatic coupling terms and conical intersections*; Wiley-Blackwell, 2006.
(13) Gomez-Carrasco, S.; Gonzalez-Sanchez, L.; Bulut, N.; Roncero, O.; Banares, L.; Castillo, J. F. State-to-state quantum wave packet dynamics of the LiH plus H reaction on two ab initio potential energy surfaces. *Astrophys. J.* **2014**, *784*, 55.
(14) Kim, K.; Lee, Y.; Ishida, T.; Jeung, G. Dynamics calculations for the LiH + H→Li + H_2 reactions using interpolations of accurate ab initio potential energy surfaces. *J. Chem. Phys.* **2003**, *119*, 4689−4693.
(15) Bovino, S.; Wernli, M.; Gianturco, F. A. Fast LiH destruction in reaction with H: quantum calculations and astrophysical consequences. *Astrophys. J.* **2009**, *699*, 383−387.
(16) Bovino, S.; Tacconi, M.; Gianturco, F. A.; Galli, D.; Palla, F. On the relative abundance of LiH and LiH^+ molecules in the early universe: new results from quantum reactions. *Astrophys. J.* **2011**, *731*, 107.
(17) Roy, T.; Mahapatra, S. Quantum dynamics of H plus LiH reaction and its isotopic variants. *J. Chem. Phys.* **2012**, *136*, 174313.
(18) He, X.; Wu, H.; Zhang, P.; Zhang, Y. Quantum state-to-state dynamics of the H + LiH→H_2 + Li reaction. *J. Phys. Chem. A* **2015**, *119*, 8912−8921.
(19) Brouard, M.; Vallance, C. *Tutorials in Molecular Reaction Dynamics*; The Royal Society of Chemistry: Cambridge, 2010.
(20) Liu, Y. F.; He, X. H.; Shi, D. H.; Sun, J. F. Theoretical study of the dynamics for the H + LiH(v = 0, j = 0)→H_2 + Li reaction and its isotopic variants. *Eur. Phys. J. D* **2011**, *61*, 349−353.
(21) Liu, Y.; He, X.; Shi, D.; Sun, J. Stereodynamics of the reaction H + LiH(v = 0, j = 0)→H_2 + Li and its isotopic variants. *Comput. Theor. Chem.* **2011**, *965*, 107−113.
(22) Wang, Y.; Zhang, J.; Jiang, Y.; Wang, K.; Zhou, M.; Liang, X. Investigation of stereo-dynamic properties for the reaction H plus HLi by quasi-classical trajectory approach. *Bull. Korean Chem. Soc.* **2012**, *33*, 2873−2877.
(23) Zhai, H.-S.; Yin, S.-H. Stereo-dynamics of the exchange reaction $H_a + LiH_b \rightarrow LiH_a + H_b$ and its isotopic variants. *Chin. Phys. B* **2012**, *21*, 128201.
(24) Li, D.; Wang, Y.; Wang, J.; Zhao, Y. Influence of collision energy and reagent vibrational excitation on the dynamics of the reaction H plus LiH. *Int. J. Quantum Chem.* **2013**, *113*, 2379−2384.
(25) Jiang, Z.; Wang, M.; Yang, C.; He, D. Influence of collision energy and reagent vibrational excitation on the stereodynamics of the reaction H + LiH→H_2 + Li. *Chem. Phys.* **2013**, *415*, 8−13.
(26) Aldegunde, J.; Aoiz, F. J.; de Miranda, M. P. Quantum mechanical limits to the control of atom-diatom chemical reactions through the polarisation of the reactants. *Phys. Chem. Chem. Phys.* **2008**, *10*, 1139−1150.
(27) Sha, G.; Yuan, J.; Meng, C.; Chen, M. Influence of early-staged energy barrier on stereodynamics of reaction of LiH(v = 0, j = 0) + H →Li + H_2. *Chem. Res. Chin. Univ.* **2013**, *29*, 956−961.
(28) Gomez-Carrasco, S.; Roncero, O. Coordinate transformation methods to calculate state-to-state reaction probabilities with wave packet treatments. *J. Chem. Phys.* **2006**, *125*, 054102.
(29) Wigner, E. P. On the behavior of cross sections near thresholds. *Phys. Rev.* **1948**, *73*, 1002−1010.
(30) de Miranda, M.; Clary, D. Quantum dynamical stereochemistry of atom-diatom reactions. *J. Chem. Phys.* **1997**, *106*, 4509−4521.
(31) Zare, R. N. *Angular Momentum*; John Wiley & Sons, 1987.
(32) Aldegunde, J.; de Miranda, M.; Haigh, J.; Kendrick, B.; Saez-Rabanos, V.; Aoiz, F. How reactants polarization can be used to change and unravel chemical reactivity. *J. Phys. Chem. A* **2005**, *109*, 6200−6217.
(33) Aldegunde, J.; Alvariño, J.; de Miranda, M.; Sáez-Rábanos, V.; Aoiz, F. Mechanism and control of the F + H_2 reaction at low and ultralow collision energies. *J. Chem. Phys.* **2006**, *125*, 133104.
(34) Aldegunde, J.; Herraez-Aguilar, D.; de Jambrina, P.; Aoiz, F.; Jankunas, J.; Zare, R. N. H + D_2 reaction dynamics in the limit of low product recoil energy. *J. Phys. Chem. Lett.* **2012**, *3*, 2959−2963.
(35) Greaves, S. J.; Wrede, E.; Goldberg, N. T.; Zhang, J.; Miller, D. J.; Zare, R. N. Vibrational excitation through tug-of-war inelastic collisions. *Nature* **2008**, *454*, 88−91.

DOI: 10.1021/acs.jpca.6b10094
J. Phys. Chem. A 2017, 121, 1535−1543